Implementation and verification of the Hybrid Transformer model in ATPDraw

Hans K. Høidalen, Bruce A. Mork, Francisco Gonzalez, Dmitry Ishchenko, Nicola Chiesa

Abstract-- The paper documents a new transformer model in ATPDraw called XFMR. This model handles 3-phase transformers with two or three windings. Autotransformers and all Wye and Delta couplings are supported. The model includes an inverse inductance matrix for the leakage description, optional frequency dependent winding resistance, capacitive coupling, and a topologically correct core model (3- and 5-legged) with individual saturation and losses in legs and yokes. Three different sources of data are supported; typical values, standard test reports, and design information. The hybrid model XFMR is compared to the UMEC model in PSCAD showing good agreement at rated, stationary operation, but considerable differences in transient situations. Both models need development to reproduce all switching transient behaviors properly.

Keywords: Transformer modeling, saturation, leakage inductance, winding resistance, capacitance, topologically correct core.

I. INTRODUCTION

THE transformer is an essential component in power systems but the standard models used to represent it in transient analysis are rather poor. Several approaches are documented in the literature [1] and this paper focuses on models with topologically correct cores. A model called the Hybrid Transformer model [2]-[4] is recently implemented in ATPDraw and is there called XFMR. The characteristics and implementation of this model is outlined in this paper and its response is compared to the UMEC model [5], [6] found in PSCAD. UMEC is chosen since it is based on similar core geometry data as XFMR. The purpose is not to show which model is the best but rather to point out the need for improved transformer models for switching transient studies.

II. MODELING

The modeling of the transformer is based on the magnetic circuit transformed to its electric dual [2], [3]. The leakage and main fluxes are then separated into a core model for the main flux and an inverse inductance matrix for the leakage flux. The copper losses and coil capacitances are added at the terminals of the transformer. The resulting electrical circuit is shown in Fig. 1. Only standard EMTP elements are used.
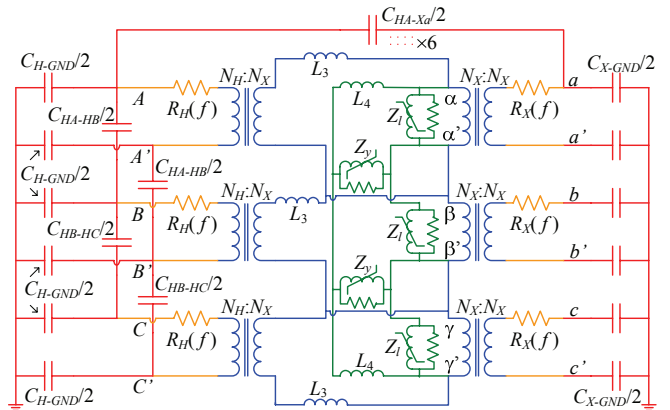
Fig. 1. Electric model of the Hybrid Transformer [4], 2-windings (H and X), 3-phases, 3-legged core.

Modeling of the transformer can be based on three different data sources; typical values, test report, and design information. The three sources can be selected independently for resistance, inductance, capacitance, and core. Test report input is based on standard open and short circuits tests, with capacitance measurements as an additional option. This is the normal choice of data source for existing transformers. Design data requires the geometry and material parameters of the windings and the core. Such data are rarely available so this option is more for research purposes. The Typical value option uses available text book tabulated values of leakage impedance, copper and core losses, and magnetizing current to estimate a transformer model. This is suitable when the transformer is not purchased yet, or data is unavailable in an initial study. However, such model must be used with caution.

A. Leakage inductance

The leakage inductance is modeled with an inverse inductance matrix (A-matrix). The matrix has dimension $(nw+1) \cdot np$ where nw is the number of physical windings, the core is connected to the $nw +1$ winding, and np is the number of phases [2], [3], [7]. The coupling (auto, Y, D) and phase shift is produced directly in the A-matrix. All possible phase shifts are supported. The A-matrix has the following structure for a three-winding, three-phase transformer:

$$A = \begin{array}{cc} \begin{array}{ccc} A & B & C \end{array} \\ \begin{bmatrix} A_w & 0 & 0 \\ 0 & A_w & 0 \\ 0 & 0 & A_w \end{bmatrix} \end{array} \text{ where } A_w = \begin{array}{cc} \begin{array}{cccc} P & S & T & C \end{array} \\ \begin{bmatrix} a_{11} & a_{12} & a_{13} & a_{14} \\ a_{21} & a_{22} & a_{23} & a_{24} \\ a_{31} & a_{32} & a_{33} & a_{34} \\ a_{41} & a_{42} & a_{43} & a_{44} \end{bmatrix} \end{array} \quad (1)$$

where ABC are the three phases and PSTC stands for primary, secondary, tertiary, and the core ($nw+1$) winding.

The *A*-matrix is assumed to have no mutual coupling between the phases. The entire zero-sequence effect is modeled in the attached core. The A_w-matrix is established according to the EMTP Theory Book [8] chapt. 6.4, and section 5.2.4 p. 31 in [2].

1) Typical values

The leakage reactance is established from [9] using the lowest value in the typical range. In the case of a three-winding transformer the leakage reactance (in pu) between the inner and outer winding is approximated as the sum of the other two. In this case it is assumed that the medium voltage winding is the middle one.

2) Test report

The leakage reactance is calculated from the standard test report short circuit data (positive sequence).

$$X[pu] = \sqrt{Z[\%]^2 - (P[kW]/(10*S[MVA]))^2} /100 \qquad (2)$$

In the case of an autotransformer the reactances are scaled according to the Theory Book [8] chapt. 6.7.

3) Design data

The leakage reactances are calculated according to classical MMF distribution theory as shown in [2], [3]. Both cylindrical and pancake windings are supported.

4) Handling of the core winding

The artificial core winding is related to the leakage channel between the inner physical winding and the core. A parameter $K=a_1/a_2$ is defined in [2], [7] where a_1 is the width of the inner leakage channel and a_2 is the width of the leakage channel between the inner and the outer/middle winding. A fixed value $K=0.5$ is used in ATPDraw. If the pu leakage reactances X_{ML}, X_{MH}, and X_{HL} (*L*=inner, *M*=middle, *H*=outer) for a three winding transformer are given then the leakage reactances to the core winding are assumed to be [2], [7]

$$X_{LC} \approx K \cdot X_{ML}, X_{MC} \approx X_{LC} + X_{ML} = (K+1) \cdot X_{ML}, \text{ and}$$
$$X_{HC} \approx X_{MC} + X_{HM} = (K+1) \cdot X_{ML} + X_{HM} \qquad (3)$$

B. Winding resistance

The winding resistances are added externally at the terminal of the transformer (*A*-matrix). Optionally, the resistances can be frequency dependent.

1) Typical values

The typical winding resistances (at power frequency) are in principle based on [10]. A function (4) is established that takes in the parameter *u* [kV] and *s* [MVA] and returns the resistance in %. Data for a 290 MVA/ 420 kV transformer (Tab. I) were used to extend the data given in [10]:

$$Rw = 0.7537 \cdot \left(\frac{u}{15}\right)^{0.0859} \cdot s^{-0.2759} \ [\%] \qquad (4)$$

2) Test report

The test report data are given at power frequency. The per unit short circuit resistances are calculated from short circuit power losses in the test report (positive sequence). The winding resistance (in pu) is assumed to be equally shared between the windings in the case of a two-winding transformer. In the case of a 3-winding transformer the traditional star-equivalent approach is used.

In the case of an auto-transformer the short circuit resistances are recalculated according to the power balance used in [7]. The approach used for reactances (from the Theory Book [8]) did not work out for the resistances.

3) Design data

The user can specify the winding conductivity σ, the equivalent cross section *A* of each turn, the average length *l* of each turn, number of turns of the inner winding *N*. The DC resistance is normalized to the power frequency. If the resistance is assumed to be frequency dependent the conductor area must be specified in height and width (which determines the stray losses).

4) Frequency dependency

The frequency dependent resistance is calculated between 0.1 to 10 kHz. The typical values and test report resistances are assumed to follow $R(\omega) = R_0 \cdot \sqrt{\omega/\omega_0}$ where R_0 is the resistance at the angular power frequency ω_0. This expression results in considerably lower values than suggested in Fig. 26 in [2]. This needs to be further investigated. The design data resistances are assumed to follow eq. (37) in [2].

The calculated $R(\omega)$ and ω value pairs are fitted to the function (two-cell Foster equivalent [11])

$$R(\omega) = R_0 + \frac{R_1 \cdot \omega^2 \cdot L_1^2}{R_1^2 + \omega^2 \cdot L_1^2} + \frac{R_2 \cdot \omega^2 \cdot L_2^2}{R_2^2 + \omega^2 \cdot L_2^2} \qquad (5)$$

with the resistances R_1 and R_2, and inductances L_1 and L_2 as unknowns. The fitting routine is based on the Lavenberg-Marquardt method and a simplified version of `mrqmin` from ref. [12]. A negative inductance $L_0=-L_1-L_2$ is added in series to the winding resistance to compensate for the inductance of the Foster cells. A constraint is put on the total inductance $|L_0| < L_w$ where L_w is the inverse of the diagonal A_w-matrix element, [2] section 5.4.2. The constraint is handled simply by setting $L_1=L_2=0.5 \cdot L_w$ when the constraint is violated and then continue to obtain new optimized values for R_1 and R_2.

C. Capacitance

The *C*-matrix is split in two halves and connected to each end of the physical windings. The capacitance matrix *C* is based on the following two matrices:

$$C_w = \begin{bmatrix} C_{11} & C_{12} & C_{13} \\ C_{21} & C_{22} & C_{23} \\ C_{31} & C_{32} & C_{33} \end{bmatrix} \text{ and } C_p = \begin{bmatrix} C_{AA} & C_{AB} & C_{AC} \\ C_{BA} & C_{BB} & C_{BC} \\ C_{CA} & C_{CB} & C_{CC} \end{bmatrix} \qquad (6)$$

The C_w matrix contains the capacitances between windings 1-3 equal in all phases. The capacitance matrix C_w is built up like a nodal admittance matrix. The C_p matrix contains capacitances that are specific to phase A, B, or C. These are typically connected to the outer windings. The total *C*-matrix is then built on these two symmetrical matrices dependent on the type of winding (pancake/cylindrical). The concept 'outer winding' will be different for pancake and cylindrical windings.

1) Typical values

A capacitive coupling factor K_c can be specified by the user with a default value of 0.3. The concept of transient recovery voltage (TRV) is used to calculate the effective capacitance when the inductance is known [13]. IEEE standard C37, Fig. B2 [14] is used to obtain the typical frequency of the TRV for a known voltage level and fault current.

$$C_{eff}(U,S,X_{pu},f) = \frac{f}{2\pi} \cdot \frac{3 \cdot I}{U \cdot (f_{TRV}(U,I))^2} \ [\mu F] \tag{7}$$

with U in [kV], S in [MVA] and $I = \dfrac{S}{3 \cdot U \cdot X_{pu}}$ [kA]

In the case of typical values, the C_p matrix (between phases) is always set to zero for lack of any better choice. For a two-winding transformer the C_w matrix is calculated as

$$C_w[1,2] = C_{PS} = K_c \cdot C_{eff}(U_S,S,X_{PS,pu},f)$$
$$C_w[1,1] = C_{PP} = C_{eff}(U_P,S,X_{PS,pu},f) - C_w[1,2] \tag{8}$$
$$C_w[2,2] = C_{SS} = (1/K_c - 1) \cdot C_w[1,2]$$

For a three winding transformer the typical capacitance is more complicated with several coupling factors involved. Here a simple approach is used:

$$C_w[1,3] = C_{PT} = 0$$
$$C_w[2,3] = C_{ST} = C_{eff}(U_S,S,X_{ST,pu},f) - C_w[2,2] \tag{9}$$
$$C_w[3,3] = C_{TT} = C_{eff}(U_T,S,X_{ST,pu},f) - C_w[2,3]$$

This approach could be further discussed and improved.

2) Test report

In the test report the capacitances between each winding and ground and between all windings is assumed to be directly specified while the C_p matrix is set to zero. All values must be specified per phase.

3) Design data

The calculation of design data capacitances are based on [2] chapt. 5.3, p. 33-42. The user has to specify the winding geometry as well as the various equivalent permittivities of insulation system. Standard formulas for calculating the capacitance between cylinders and for cylinders over plans are used with end effect and tank effect adjustments.

D. Core

The core model is connected to the artificial core winding terminal on the A-matrix. Only stacked cores with three and five legs are supported at this point. Basically the inductive and resistive core parts are treated independently. The core losses are assumed to be linear and the nonlinear inductances are modeled by the Frolich equation (10). Each part of the core is modeled with its own core loss resistance and nonlinear inductance using information about their relative cross section and length to scale the values. Fig. 2 shows the core model for a 5-legged transformer.

It is assumed that the magnetic material is characterized by four parameters a, b, d and e. A list of typical steel materials is developed based on fitting the manufacturer's data from state of the art catalogues. Older steel materials will have a different characteristic and the losses are typically higher. The material list is only used for design data and typical values.
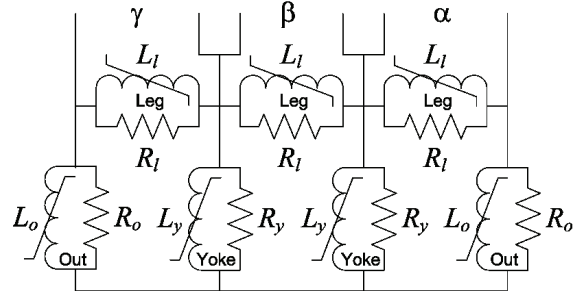
Fig. 2. 5-legged stacked core model. The αβγ terminals are the $nw+1$ winding.

The B/H relationship is assumed to follow the Frolich

equation $B = \dfrac{H}{a + b \cdot |H|}$ (10)

The specific loss is assumed to follow

$$p\ [W/kg] = \left(\frac{f}{50}\right)^{1.5} \cdot \left(d \cdot B^2 + e \cdot B^{10}\right) \tag{11}$$

where f is the power frequency.

The specific loss is traditionally (for instance Westinghouse T&D reference book, 1964) assumed to be $p = K_e \cdot (f \cdot t \cdot B_{max})^2 + K_e \cdot f \cdot B_{max}^x$ with x said to be 3 for modern materials in the year of 1964. In the above expression t is the thickness of the laminates. The traditional expression was tested on modern material data with little success.

Fig. 3 shows the fit of the specific losses and DC-magnetization curve of ARMCO M4 steel. The Frolich fitting is not very good, and in Fig. 3b fitting around the knee point (nominal flux) was preferred at the sacrifice of high field fitting (B=1.9 T). Similar fitting is performed for the other core materials. A modification of the Frolich equation which improves the agreement is introduced in [15]. This method is implemented in ATPDraw but is not described here since the numerical implementation of this method still needs improvement.
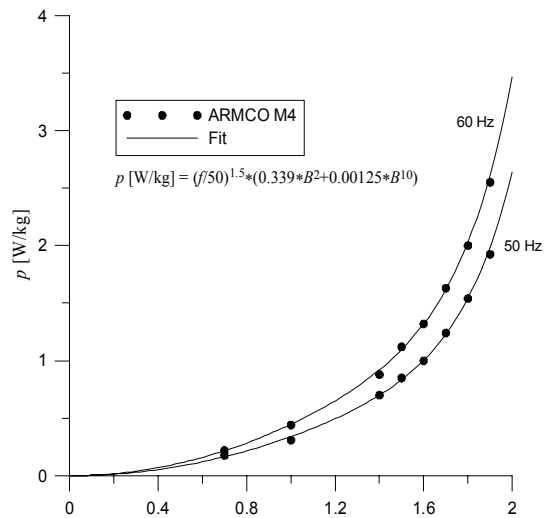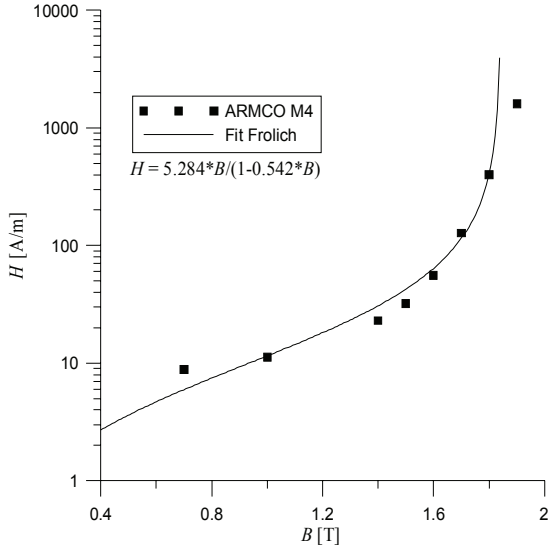
Fig. 3 a) Core loss curves

Fig. 3 b) DC-magnetization curve

The chart shows ARMCO M4 data points and Fit Frolich curve with equation $H = 5.284 \cdot B/(1-0.542 \cdot B)$, with axes H [A/m] (logarithmic, 1 to 10000) and B [T] (0.4 to 2).

Inductance modeling:

The basic Frolich equation in (10) is reformulated as a current flux-linkage characteristic by introducing the flux linkage $\lambda = B \cdot A \cdot N$ and the current $i = H \cdot l / N$ where N is the number of turns of the inner winding, A is the cross section, and l is the length of the involved core section. This gives

$$\lambda = \frac{i \cdot A \cdot N^2 / l}{a + b \cdot |i| \cdot N / l} = \frac{i \cdot A_r}{a' \cdot l_r + b' \cdot |i|} \tag{12}$$

where *the* constants $a' = a \cdot l_L /(N^2 \cdot A_L)$ and $b' = b/(N \cdot A_L)$, based on the absolute length (l_L) and cross section area (A_L) of the core leg, are determined in an optimization process.

The final characteristics are determined by inserting the relative dimensions for the corresponding section, A_r and l_r. The nonlinear inductances are implemented as optional type 93 or type 98 inductances in ATP.

Core loss modeling

The core loss is split in parts associated with individual core sections. If we assume that the core loss is proportional to the volume of the core we can set the outer leg (R_o) and yoke resistances (R_y) proportional to the leg resistance (R_l):

$R_o = R_l /(A_{rl} \cdot l_{rl})$ and $R_y = R_l /(A_{ry} \cdot l_{ry})$ where l_r and A_r are the relative dimensions. Based on the resistive part of Fig. 2 this gives the total core loss as inverse proportional to the leg resistance R_l. The constant $K_{3/5}$ is dependent on the core geometry.

$$P_{loss} = \frac{V^2}{R_l} \cdot K_{3/5} \tag{13}$$

1) Typical values

The estimation of the magnetizing current (I_m) is based on [10]. Some fitting of the data is performed which results in

$$I_m = 0.73 \cdot \left(\frac{BIL}{350}\right)^{0.2933} \cdot \left(\frac{s}{20}\right)^{-0.2154} \quad [\%] \tag{14}$$

when the basic insulation level (*BIL*) is known and

$$I_m = 0.855 \cdot \left(\frac{u}{150}\right)^{0.2283} \cdot \left(\frac{s}{20}\right)^{-0.2134} \quad [\%] \tag{15}$$

when *BIL* must be estimated. *BIL* is in [kV], *u* is the rated voltage in [kV] and *s* is the rated power in [MVA].

For a typical core model the user has to specify the maximum *B*-field (normally 1.5-1.7 Tesla) and the maximum core loss density. First a core material has to be guessed and this gives the *a* and *b* values in the Frolich equation (and possibly also the *c* and *d* values that would replace *p*).

The following relations are then assumed:

$$\lambda_{max} = \frac{\sqrt{2} \cdot U_{rms}}{\omega} = B_{max} \cdot A \cdot N \Rightarrow A \cdot N = \frac{\sqrt{2} \cdot U_{rms}}{\omega \cdot B_{max}} \tag{16}$$

$$H_{max} = \frac{a \cdot B_{max}}{1 - b \cdot B_{max}} \approx \sqrt{2} \cdot i_{rms} \cdot \frac{N}{l}$$

$$\Rightarrow \frac{N}{l} = \frac{a \cdot B_{max}}{(1 - b \cdot B_{max}) \cdot \sqrt{2} \cdot i_{rms}} \tag{17}$$

which somewhat doubtfully assumes a sinusoidal magnetizing current.

This gives the parameter of the fluxlinkage-current characteristic:

$$a' = a \cdot \frac{l}{A \cdot N^2} \approx \omega \cdot (1 - b \cdot B_{max}) \cdot \frac{i_{rms}}{u_{rms}} \quad \text{and}$$

$$b' = b \cdot \frac{1}{A \cdot N} \approx b \cdot \frac{\omega \cdot B_{max}}{\sqrt{2} \cdot u_{rms}} \tag{18}$$

We see that the expressions for *a'* and *b'* are independent of the magnetic material property *a*. The typical value of *b* seems to be fairly constant for standard core materials and a value of 0.5 is assumed in ATPDraw.

The core loss is estimated to

$$P_{loss} = p \cdot \rho \cdot A \cdot l = p \cdot \rho \cdot \frac{(1 - b \cdot B_{max}) \cdot 2 \cdot u_{rms} \cdot i_{rms}}{\omega \cdot a \cdot B_{max}^2} \tag{19}$$

where p [W/kg] and ρ [kg/m^3] are given and the volume $A \cdot l$ is estimated from (16) and (17).

2) Test report

The user specifies the excitation voltage in [%], the current in [%] and the core loss in [kW]. The core loss is used directly as explained above to obtain the core resistances. At the moment the core resistances are assumed to be linear and the core loss value at 100 % excitation is used.

The inductive magnetizing current for each point is calculated as

$$I_{rms} = \sqrt{I_0[\%]^2 - \left(\frac{P[kW]}{10 \cdot S[MVA]}\right)^2} \quad [\%] \tag{20}$$

This results in a sequence of excitation points (U_{rms} and I_{rms}). The magnetic circuit in Fig. 2 assuming sinusoidal fluxes is solved and the rms values of the line currents are calculated and compared to measured ones. Optimized values of *a'* and *b'* in (12) are found by a constrained Golden Search [12] optimization method implemented in ATPDraw [15]. If a single point is specified the core model is linear.

3) Design data

For design data the user specifies the core material directly with its B-H relationship (*a* and *b* values in (10)). The absolute core dimensions and the number of inner-winding turns *N* are known, so the inductances can be found directly from (12). Based on manufacturer data the core losses can be established from (11) with $B = \dfrac{\sqrt{2} \cdot U_{rms}}{\omega \cdot A \cdot N}$ and known values of the core weight (volume and density) the core loss can be estimated.

III. VERIFICATION

This section shows a comparison between the new XFMR model and the UMEC model. Version 4.1 of PSCAD and version 5.0 of ATPDraw were used for the modeling. The test object used in this paper is a 290 MVA generator step-up transformer with a 5-legged stacked core. Some limited core design information was available. The yoke and outer leg area is 0.54 times the leg area. The yoke and outer leg lengths are approximately 1.5 and 2.5 times the leg length. Table I shows the test report data for the transformer.

TABLE I
GENERATOR STEP-UP TRANSFORMER TEST REPORT

Main data	[kV]	[MVA]	[A]	Coupling
HS	432	290	388	YNj
LS	16	290	10465	d5
Open-circuit	E_0 [kV,(%)]	[MVA]	I_0 [%]	P_0 [kW]
LS	12 (75)	290	0.05	83.1
	14 (87.5)	290	0.11	118.8
	15 (93.75)	290	0.17	143.6
	16 (100)	290	0.31	178.6
	17 (106.25)	290	0.67	226.5
Short-circuit	[kV]	[MVA]	*ek, er* [%]	P_k [kW]
HS/LS	432/16	290	14.6, 0.24	704.4

TABLE II
CALCULATED λ/i −CHARACTERISTICS FOR UMEC INPUT

λ [pu]	i_Z [%]	i_L [%]	$i_\Delta \cdot \sqrt{3}$ [%]
0.75	0.0707	0.0580	0.0707
0.875	0.2224	0.2120	0.2386
0.9375	0.3590	0.3486	0.3995
1.0	0.7170	0.7085	0.8268
1.0625	1.6509	1.6446	1.9582

For the UMEC model the test report I_0-E_0 open circuit data are converted into a peak current and fluxlinkage characteristic externally since this was not a feature of this model. In this process the loss component was subtracted and the harmonics in the line current of the delta-winding handled with 3pl-harmonic elimination [16], [17] using the phase current. Table II shows the calculated values (i_Z directly from I_0 in Tab. I, i_L after subtraction of the losses, and i_Δ is the phase current in the delta with 3-pl harmonic elimination). In order to meet the UMEC model requirements the peak-current was divided by $\sqrt{2}$ and scaled back to line currents with $\sqrt{3}$. Without the proper handling of the delta winding the UMEC model produced too small magnetization current. For both models the core loss is assumed to be constant at the rated

value even if the test report shows nonlinearity. The UMEC model did not support the phase shift (150 deg.) specified for the tested transformer and this has been handled by using a lead-coupling and renaming the current abc to cab.

Figure 4 shows the open circuit test report values and the corresponding rms quantities calculated in PSCAD and ATP. The voltage is applied on the LS side and the source has zero impedance. The average current values were established by RMS tools available in the two programs. At values below rated voltage the two models correspond fairly well to each other and to the test report, while at higher excitations there is a substantial difference. The XFMR model uses a Frolich equation that goes into complete saturation (the current is leakage reactance limited), while the UMEC model uses a linear extrapolation.
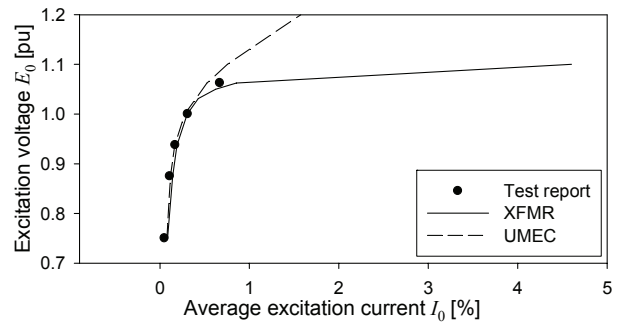

Fig. 4. Test report values compared to calculated quantities for the XFMR and UMEC models.
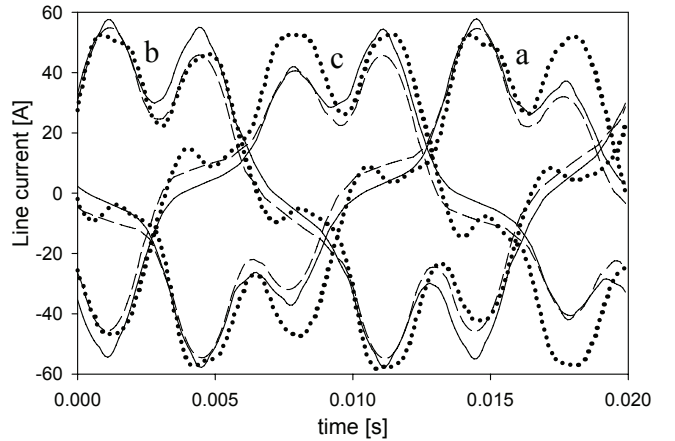

Fig. 5. Measured and calculated magnetization current. Solid lines: XFMR, dashed lines: UMEC, dotted lines: Measurements.

For the test object some waveform records of the excitation current were available. Figure 5 shows the comparison between the XFMR, the UMEC model and measured magnetization current at rated voltage. Generally, the XFMR current is a bit higher than the UMEC current peaks. Phase b is better reproduced by the UMEC model. We also see that the measured current is not symmetrical for some unknown reason. The model assumption of equal core sections is not necessarily true, as well as the exact core length ratios were not known. We also see some strange behavior around zero

crossing of the current which can be due to a non-sinusoidal excitation voltage.

Figure 6 and 7 show calculated XFMR and UMEC response of circuit breaker (CB) operation on the LS side (the HS is open). The applied voltage was also in this case ideal with rated value (16 kV). Figure 6 shows the calculated fluxlinkage for the XFMR and UMEC models. We see a small difference during the ring-down transient period, but otherwise the fluxes are almost identical. Fig. 7 shows the calculated inrush currents where the XFMR model gives around 20 times higher values than the UMEC model. This can be explained from Fig. 4 and the large differences at extreme saturation. The reality is probably somewhere in between the XFMR and UMEC models, but the XFMR model seems to have a more realistic shape of the saturation curve.
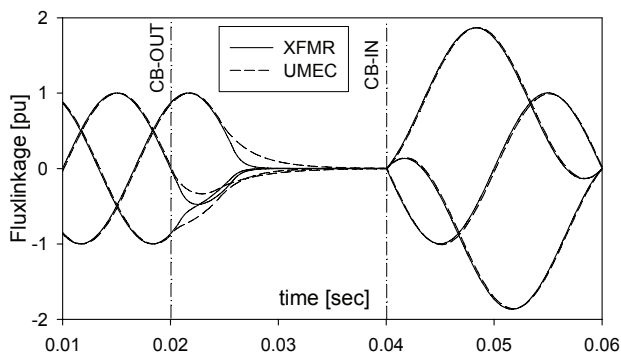

Fig. 6. Calculated fluxlinkages for the XFMR and UMEC models. For the XFMR model the flux is found by an integration of the LS line voltages.
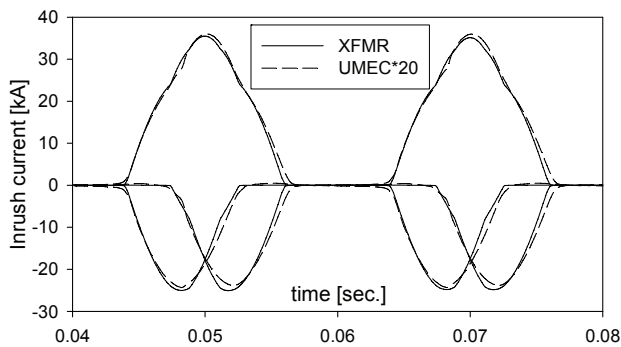

Fig. 7. Calculated inrush line currents for the XFMR and UMEC models.

IV. CONCLUSION

The XFMR and UMEC models give fairly the same result at steady state and rated voltage. The most important difference is seen in Fig. 4. The XFMR core model uses a Frolich equation that goes into complete saturation, while the UMEC model uses a linear extrapolation. This results in very different over-excitation responses and inrush currents. The UMEC model requires substantial manual conditioning of the open circuit test report data as shown in Tab. II. Both models need to be developed in order to reproduce all kinds of switching transients. The representation of extreme saturation, zero-sequence, nonlinear core losses, hysteresis, and remanence should be added.

V. REFERENCES

[1] J. A. Martinez and B. A. Mork, "Transformer modeling for low- and mid-frequency transients – a review", *IEEE Trans. Power Delivery*, vol. 20, no. 2, pp. 1625-1632, 2005.

[2] B. A. Mork, F. Gonzalez, and D. Ishchenko: "Parameter estimation and advancements in transformer models for EMTP simulations. Task MTU-7: Model performance and sencitivity analysis", Bonneville Power Administration, Portland, OR, 2004.

[3] B.A. Mork, F. Gonzalez, D. Ishchenko, D. L. Stuehm, J. Mitra." Hybrid Transformer Model for Transient Simulation-Part I: Development and Parameters", *IEEE Trans. Power Delivery*, Vol. 22, pp. 248-255, 2007.

[4] B.A. Mork, F. Gonzalez, D. Ishchenko, D. L. Stuehm, J. Mitra, "Hybrid Transformer Model for Transient Simulation-Part II: Laboratory Measurements and Benchmarking", *IEEE Trans. Power Delivery*, Vol. 22, pp. 256-262, Jan. 2007

[5] W. Enright, O. Navak, G. Irwin, and J. Arrillaga, "An electromagnetic transients model of multi-limb transformers using normalized core concept", in *Proc. 1997 Int. conf. Power System Transients*, pp. 93-98.

[6] W. Enright, O. Navak, and N. Watson, "Three-phase five-limb unified magnetic equivalent circuit transformer models for pscad v3", in *Proc. 1999 Int. conf. Power System Transients*, pp. 462-467.

[7] B. A. Mork, F. Gonzalez, D. Ichshenko, "Leakage inductance model for Autotransformer transient simulation", in *Proc. Int. Conf. on Power System Transients*, paper 248, 2005.

[8] H. W. Dommel and et.al., *Electromagnetic Transients Program Reference Manual (EMTP Theory Book)*, Portland, OR: Prepared for BPA, Aug. 1986.

[9] J. J. Graininger and W. D. Stevenson: *Power System Analysis*, McGraw-Hill 1994.

[10] A. Greenwood: *Electrical Transients in Power Systems*, Wiley, 1991.

[11] F. deLeon, A. Semlyen, "Time domain modeling of eddy current effects for transformer transients", *IEEE Trans. Power Delivery*, vol. 8, no. 1, pp. 271-280, 1993.

[12] W. H. Press, S. A. Teukolsky, W. T. Vetterling, B. P. Flannery: *Numerical recipes in Fortran*, 2nd ed. Cambridge University Press, 1992.

[13] IEEE Working Group 15.08.09, Editors: A. M. Gole, J. Martinez-Velasco, A. J. F Keri, *Modeling and analysis of power system transients using digital programs*, IEEE 99TP133-0, pp. 4.12-4.13, 1998.

[14] *IEEE Guide for Transient Recovery Voltage for AC High-Voltage Circuit Breakers Rated on a Symmetrical Current Basis*, ANSI/IEEE Standard C37.011-1994.

[15] N. Chiesa, "Power Transformer Modelling: Advanced Core Model", M. SC. Thesis, Politecnico di Milano, Italy, 2005.

[16] W. L. A. Neves and H. W. Dommel, "Saturation curves of delta-connected transformers from measurements", *IEEE Trans. Power Delivery*, vol. 10, no. 3, pp. 1432-1437, 1995.

[17] N. Chiesa, H. K. Høidalen, "On the calculation of fluxlinkage/current-characteristics for Δ-coupled transformer winding", presented at the European EMTP User Group meeting in Warzaw-Poland, 2005.

VI. BIOGAPHIES

Hans Kr. Høidalen was born in Norway in 1967. He received his MSc and PhD from the Norwegian University of Science and Technology in 1990 and 1998 respectively. He is now a professor at the same institution with a special interest of electrical stress calculations and modeling.

Bruce A. Mork was born in ND-USA in 1957. He received the BSME, MSEE, and PhD from North Dakota State University in 1979, 1981 and 1992 respectively. He joined the faculty of Michigan Technological University in 1992, where he is now Associate Professor of Electrical Engineering, and Director of the Power & Energy Research Center.

Francisco Gonzales was born in Spain. He received the M.S. and PhD from Universitat Politècnica de Catalunya in 1996 and 2001 respectively. He worked as Postdoc at Michigan Technological University from 2002 to 2005. He is now with El Sewedy Cables in Egypt.

Dmitry Ishchenko was born in Krasnodar, Russia. He received his M.S. and PhD degrees in Electrical Engineering from Kuban State Technological University, Russia in 1997 and 2002 respectively. In 2003 he joined Michigan Techological University as a postdoctoral researcher.

Nicola Chiesa was born in Italy in 1980. He received the M.Sc. degree in electrical Engineering from Politecnico di Milano in 2005. In Sept. 2005 he joined the Norwegian University of Science and Technology as a PhD candidate.